CHAPTER IV
ELECTRICAL CONDUCTIVITY RESPONSE OF POLYPYRROLE/MOLECULAR SIEVE 13X COMPOSITES TO CH_4, CO_2, CO, AND SO_2: EFFECTS OF CATION TYPE AND CATION CONCENTRATION

Abstract

Electrical conductivity sensitivity of polypyrrole(Ppy)/molecular sieve 13X composites exposed to CH_4, CO_2, CO, and SO_2 was investigated. Composites were prepared by a dry mixing and dispersion. Effects of zeolite concentration , cation type, concentration of cation were investigated. The electrical conductivity of Ppy doped with naphthalene-2-sulfonic acid(β) sodium salt varies monotonically with the doping level. There is no electrical conductivity response when Ppy and its composites are exposed to CH_4, CO_2, and CO in contrast to the Ppy exposed to SO_2. Undoped Ppy and doped Ppy composites at 10% v/v of 13X content possess the highest sensitivity to SO_2; the sensitivity is reduced as molecular sieve 13X content increases. Cation-exchanged processes on the molecular sieve 13X were carried out by changing from Na^+ to Li^+, K^+, and Cs^+ at various amounts The composites of unmodified 13X in which Na^+ is fully present give the greatest sensitivity to SO_2. The sensitivity of Ppy/13X composite to SO_2 is reduced by exchanging cation in molecular sieve13X from Na^+ to other alkali cations in this decreasing order: Cs^+, K^+, and Li^+.

Keywords: Conducting polymer, polypyrole, gas sensor, molecular sieve 13X

1. Introduction

Conductive polymers, generally composed of conjugated monomer units with π-electrons delocalized along the back bone, have been utilized in various applications. Conductive polymers have many advantages over metallic counterparts: low cost materials, simple fabrication techniques, easy deposition on various substrates, and flexible molecular architectures[1]. The electrical conduction properties of conductive polymers are controlled by the addition of a small quantity of foreign molecules into the host polymer matrix. Both n- type and p-type dopants have been utilized to induce an insulator-metal transition in conductive polymers[2]. Due to the thermodynamic stability of intermediates, one of carbocation is greater than one of carbanion, conductive polymers are usually doped by a p-type dopant[3]. Polypyrole (Ppy), one of conductive polymers, has been investigated and developed towards gas sensing applications because it can be easily synthesized[1] and it possesses excellent thermal and electrical properties. Ppy is normally polymerized by either an electrochemical method[4-6] or a chemical method[7-10]. However, Ppy has low selectivity for a particular gas, poor mechanical property, and inefficient solubility[1]. To improve these disadvantages, many fundamental studies have been conducted[11-13]. Toxic and flammable gases such as CO, SO_2, NH_3, ethanol, and acetone, have been chosen and investigated as target gases to be detected by conductive polymers[1,3,14]. The effects of dopant, temperature, and concentration of dopant on Ppy have been studied in order to achieve the highest conductivity response and the lowest gas detection limit[11,15-19]. CO, NO_2, and SO_2 are typically emitted by the combustion of fossil fuels in factories and from automobile engines, causing environmental problems and vitally affecting human heaths[20-22]. In principle, these gases are expected to be detectable by Ppy because they act as electrophilic gases, withdrawing electrons from the polymer[1,23].

In the gas separation and gas purification fields, zeolite molecular sieves are well known for a wide variety of applications, in particular their superior selective adsorption properties[23]. The absorption properties of zeolite are governed by the pore size, the zeolite type, the temperature, and the cation residing in the framework. The alkali and alkaline earth cations, one of the governing absorption factors, is known to

have an electrostatic interaction with CO. For the alkali cations, the affinity to CO is in this order, Li^+, Na^+, K^+, Rb^+, and Cs^+ [24, 25]. The composites of polyaniline and zeolite have been investigated as a CO sensor, in particular the effects of zeolite type and the effect of pore sizes[23, 26]. Therefore, it is conceivable that a Ppy/zeolite composite, with a suitable type of zeolite, a suitable pore size, a suitable cation type and an appropriate amount can be used to selectively detect a particular gas.

In this work, the effects of the molecular sieve 13X content, the cation type, and the cation concentration on the electrical conductivity response of Ppy when exposed to CH_4, CO_2, CO, and SO_2 on the conductivity response will be investigated.

2. Experiment

2.1 Materials

In the polymerization Ppy, these chemicals were used: distilled pyrrole (ACROS) as the monomer, ammoniumpersulfate (MERCK) as the oxidant, naphthalene-2-sulfonic acid(β) sodium salt (90% grade, Fluka) as the dopant, methyl alcohol (AR grade, CARLO ERBA) as the washing solution. 1-methyl-2-pyrrolidone (98% grade, Fluka) was used as the solvent for preparing solution samples for the UV-Vis spectrophotometry. Molecular sieve 13X was selected as the zeolite to be used as the minor phase for the composites fabricated. This choice is based on the results of our previous study[26]. Lithium chloride (99% grade, UNILAB), potassium chloride (99% grade, Fluka), and cesium chloride (99% grade, Fluka) were used in the cation exchange processes. Nitrogen gas (99% grade, TIG), methane (99% grade, TIG), carbondioxide (99% grade, TIG), carbon monoxide (1000 ppm, TIG), and sulfur dioxide (1000 ppm, TIG) were used as the target gases.

2.2 Polymerization of Polypyrrole

Pyrrole monomer was first purified by distillating pyrrole under a reduced pressure. Doped Ppy at various amounts of the dopant anion was chemically synthesized by the *in situ* doped oxidative coupling polymerization process

according to the method of Ruangchuay[3]. The solution of 0.6846 g (3.0 millimole) of APS in 10.0 ml deionized water was slowly added to the mixture of 1.2 millimole of the dopant anion and 1.0 ml (14.5 millimole) of pyrrole monomers in 20.0 ml deionized water. The reaction was allowed to proceed at 0°C for 2 hours. The obtained Ppy was precipitated by pouring the reaction mixture into a large excess amount of deionized water. The Ppy powder was washed several times with deionized water and methanol before drying in a vacuum at room temperature for 2 days. The synthesized product was ground and sieved with a mesh (53μm). In order to study the effect of molar ratio between the dopant anion and the pyrrole monomers (N_d/N_m), Ppy was synthesized at various amounts of β-naphthalene sulfonic acid. The N_d/N_m ratios were chosen to be 1:96, 1:48, 1:24, 1:12, 1:6, and 0:6 or undoped.

2.3 Preparation of Molecular Sieve 13X

The cation-exchanged process was carried out by immersing the molecular sieve 13X in 0.5 M LiCl, KCl, and CsCl solutions (1 g of 13X per 25 ml solution) at 80 °C for 1 hour, and then centrifuging the emulsions to separate the liquid phase from the solid phase. The molecular sieve 13X was dried in a vacuum at 80 °C for a duration of 6 hours. The concentration of each cation in 13X was varied by repeatedly successive immersions. The calcined sample was further ground and sieved with a mesh (53μm) before further use.

2.4 Composite Preparation

The molecular sieve 13X was ground and dried in a vacuum oven at 80°C for a duration of 6 hours. Each sample was pressed into a disc by a hydraulic press machine at the pressure of 58.8 kN. In order to study the effect of zeolite content, various zeolite amounts chosen were 5, 10, 20, and 40 % by volume.

2.5 Characterization

FTIR (Bruker, FRA 106/S) was used to identify the functional groups of synthesized the undoped Ppy and the doped Ppy. In addition, the interaction between CH_4, CO_2, CO, and SO_2, and Ppy samples were investigated by the FTIR technique. Samples were ground with KBr. Then samples were exposed to these gases for a period of 3 hours before spectra were taken. UV-VIS spectrophotometer (PERKIN ELMER, Lambda 10) was used to investigate the electronic structure of Ppy. The chemical composition of Ppy was determined by an elemental analyzer (PE 2400 Series II CHNS/O analyzer). The degradation temperature of Ppy was measured by a thermogrametric analyzer (Dupont, TGA 2950). An XRD (Phillips PW 1830/00 No. DY1241 Diffractometer, Rigaku) was used to investigate atomic and molecular arrangements and to determine the crystallinity of our Ppy samples. The particle sizes of molecular sieve13X samples were determined by a particle size analyzer, (Malvern Instruments Ltd. Masterizer X Version 2.15). BET (Thermo Finnigan, SORPTOMATIC1990 SIRES) was used to measure the pore size and the surface area of the molecular sieve 13X. The densities of molecular sieve 13X and Ppy were determined by a pycnometer. The amount of cation in molecular sieve13X was determined by an atomic absorption spectrophotometer (Varian, SpectrAA-300).

2.6 Electrical Conductivity Measurement and Gas Detection

The electrical conductivity of Ppy samples, exposed to 10 % CH_4, 10% CO_2, 1000 ppm of CO, and SO_2, was measured by our customized four point probe meter connected to customized gas chambers. The current through the four point was supplied by a source meter (Tektronix, PS280), and the resultant voltage was measured by an A/D converter connected with a PC. The relation used to calculate the electrical conductivity is $\sigma = (1/Rt)(1/K)$, where R is resistivity (Ω), t is the pellet thickness(cm), and K is the geometric correction factor.

3. Result and Discussion

3.1 Characterization of Polypyrole

For the highly doped polypyrrole, Ppy_1:6, the UV-Vis absorption peaks appearing at 411.59 nm can be assigned to the $\pi \rightarrow \pi^*$, and at 706.05 nm can be assigned to the bipolaron species[3].

For the undoped polypyrrole, Ppy_ud, there is no UV-Vis absorbtion peak due to the insolubility of the polymer. FTIR spectrum of Ppy_ud shows absorption peaks at 2924, 1548, 1465, 1189, 965, and 795 cm^{-1}; they can be assigned to the C-H stretching, the C=C in pyrrole ring stretching, the N-H bending, the C-H in plane bending, the C-H out of plane bending, respectively[1, 3, 9, 27-29]. For Ppy_1:6, the absorption peaks at 1537, 1450, 1166, 961, and 778 cm^{-1} can be assigned to the C=C in pyrrole ring stretching, the N-H bending, the C-H in plane bending, the C-H out of plane bending, respectively[1, 3, 27-30]. This C-H stretching absorption peak at 2924 cm^{-1} disappears from the spectrum of the doped Ppy_1:6 due to the masking of the polaron and bipolaron absorption at 8066 cm^{-1}(1eV)[1,31]. The success of doping can identified from the absorption peak around 778cm^{-1}, which is the C-H out of plane vibrations in the benzene ring of the β-naphthalenesulfonate anion[27].

Elemental analysis data of doped Ppy provide us with the doping level of the polymer as can be calculated by the S/N ratio. The doping levels of Ppy_ud, Ppy_1/96, Ppy_1/48, Ppy_1/12 and Ppy_1:6 are 0.26, 0.33, 0.35, 0.51, 0.52, respectively. The TGA thermograms of doped Ppy at various N_d/N_m ratios show that the on-set degradation temperature (T_d) increases when increasing N_d/N_m ratio. T_d increases from 231.2 to 288.8 °C as N_d/N_m is varied from 0:6 to 1:6. Our result is consistent with the result of previously published work[30] which showed that Ppy doped with naphthalene sulfonic acid possesses a good thermostability. From XRD diffraction patterns, the interplanar spacing between aromatic group can be identified with the peaks at 3.4 and 3.6 Å for the doped Ppy and the undoped Ppy, respectively. For the undoped Ppy, the d-spacing at 4.5 Å refers to the distance between neighboring pyrrole rings where the α-α' linkages are single bond[32]. For the

doped Ppy, the d-spacing at 4.1- 4.2 Å refers to the distance between neighboring pyrrole rings where the α-α' linkages are double bond[3]. The distance between two hard segments of the undoped Ppy and doped Ppy can be identified with the peaks at 5.9 and 6.9-7.2 Å, respectively; the distinct peaks are due to different counterions. The counterion of the undoped Ppy is SO_4^{2-} [3]. The counterion of the doped Ppy is NSA[32]. The degree of crystallinity can be defined as the peak area at 21.3°(4.1 Å d-spacing) divided by the total area at 9.2°, 14.1°,19.4° and 24.9°.[3] The degrees of crystallinity of Ppy_ud and Ppy_1:6 are 50.3 and 80.4, respectively, as shown in Table1.

The mean particle diameters of Ppy_ud and Ppy_1:6 were measured and found to be 34.68 ± 5.57 and 38.96 ± 1.39 μm, respectively. The densities of Ppy_ud and Ppy_1:6 are 0.798 ±0.067 and 0.769±0.040 g/cm³, respectively.

3.2 Characterization of Molecular sieve 13X

The particle size of molecular sieve 13x obtained form the particle size analyzer is 8.54 ± 0.48 μm. The density of molecular sieve 13x, as determined by the pycnometry, is 1.573 g/cm³. The Si/Al ratio of molecular sieve 13x, as provided by the manufacturer (Sigma-Aldrich), is 1.4. The ratio can be used to calculate the number of unit cells per particle of 13X, which turns out to be approximately 2.33 x 10^{10} unit cells/particle. Surface area and specific pore volume of molecular sieve 13x are 643 ± 47 m²/g and 0.343 ± 0.023 cm³/g, respectively. SEM monographs show that molecular sieve 13x particles are well dispersed in the polymer matrix.

The amounts of Li^+, Na^+, K^+, and Cs^+ in ion-exchanged molecular sieve 13x are obtained by the atomic absorption spectrophotometer In terms of % mole, it is defined as the mole ratio of Li^+, K^+, or Cs^+ to the total mole of those cations and Na^+, multiplied by 100. For molecular sieve 13x ion-exchanged with Li^+, the mole percentages obtained are 32.20, 56.81, 73.92 and 81.24. For molecular sieve 13x ion-exchanged with K^+, the mole percentages obtained are 46.59, 78.48, 88.97 and 93.50. For 13X ion-exchanged with Cs+, the mole percentages obtained are 35.34, 52.84, 56.42 and 59.74.

3.3 Electrical Conductivity Measurement

3.3.1 Electrical Conductivity of Polypyrrole in Air and N_2

Figure 1 shows that electrical conductivity increases from 9.36×10^{-2} to 6.44 S/cm as the doping level increases from 0:6 to1:6.The increase in electrical conductivity can be explained in terms of the increases in the number of charge carriers and the degree of crystallinity which influences the charge mobility[1,3]. It can be noted that the electrical conductivity of the undoped Ppy is 9.36×10^{-2} S/cm, a value which is rather high. This is because APS, the oxidant used in the polymerization process, produces HSO_4^- anions which can act also as a dopant[28]. Tables 1 and 2 summarize the electrical conductivity values of all our composites under the exposures to air, N_2, CH_4, CO_2, CO, and SO_2 at ambient pressure and room temperature. The electrical conductivity of the Ppy_ud in air is $(4.68 \pm 2.48) \times 10^{-1}$ S/cm and it decreases to $(3.96 \pm 2.48) \times 10^{-1}$ S/cm when it is exposed to N_2. The similar reductions in electrical conductivity can be found in Ppy_1:6 and other Ppy_ud/13X or Ppy_1:6/13X composites. The greater electrical conductivity values in air of all our composites can be attributed to the interaction of O_2 at the active sites, polaron or bipolaron, and the presence of moisture in air[23].

3.3.2 Electrical Conductivity Response to CH_4, CO_2, CO, and SO_2

The electrical conductivity response is defined as the difference in the steady state electrical conductivity when exposed to a target gas and that of N_2 at 1 atm and 29 ± 1 °C ($\Delta\sigma = \sigma_{gas} - \sigma_{N2}$). The electrical conductivity sensitivity is defined as the ratio between the electrical response and the electrical conductivity of the samples when exposed to pure N_2 ($\Delta\sigma/\sigma_{N2}$). Our target gases studied are 10%CH_4/N_2, 10% CO_2/N_2, 1000 ppm CO/N_2, and 1000 ppm SO_2/N_2.

The sensitivity of Ppy_ud and Ppy_1:6 when exposed to CH_4 and CO_2 is between -0.05 to 0.05, as shown in Table 1. For example, the sensitivity of Ppy_ud to CH_4 is 1.57×10^{-2}, and sensitivity of Ppy_1:6 to CH_4 is 1.06×10^{-3}. The

sensitivity values of Ppy_ud and Ppy_1:6 to CO_2 are -1.93 x 10^{-2} and 6.23 x10^{-3}, respectively. Thus Ppy_ud and PPy_1:6 do not respond to CH_4 and CO_2. This is because CH_4 and CO_2 are symmetrical molecules whose permanent dipole moments are zero Cm^{33}. Moreover, these two molecules have no vacant orbital or a lone pair electron in which the electron transfer between the gases and the polymer may occur. Thus, we can summarize that there is no interaction between Ppy and methane and CO_2.

The sensitivity values of Ppy_ud and Ppy_1:6 to CO are –2.30 x 10^{-2} and – 5.48 x10^{-2}, respectively as tabulated in Table 1. Both Ppy-ud and Ppy_1:6 show negative responses to CO. It is anticipated that CO, which acts as an electrophilic gas, should draw electrons from the polymer resulting in a positive electrical response [23, 26]. Therefore, we conclude that Ppy does not interact with or respond to CO; if there was any interaction it should be very weak and negligible.

When Ppy_ud and Ppy_1:6 are exposed to SO_2, they show a positive electrical response to SO_2. The electrical response of Ppy_ud and Ppy_1:6 are 6.71 x10^{-2} S/cm and 3.17 x 10^{-1}, respectively, as shown in Table 2. The corresponding sensitivity values are 0.246 and 0.115, respectively. Thus, the electrical response of Ppy_1:6 is greater than that of Ppy_ud but the sensitivity of Ppy_1:6 is less than that of Ppy_ud. SO_2 is an electrophilic gas which can withdraw electrons from the pyrrole rings of Ppy, resulting in the increase in the number of charge carrier and the increase of electrical conductivity. Moreover, the conductivity response is not completely reversible when SO_2 is replaced by N_2. The electrical conductivity values of Ppy_ud and Ppy_1:6 differ from their initial N_2-exposure values by 14.0 to 20.1 %. Figure 2a shows FTIR spectra of Ppy_ud before the SO_2 exposure and after 3 hours of the SO_2 exposure. There is a small absorption peak at 1395 cm^{-1} in the latter spectrum which can be identified as the S=O asymmetric stretching of SO_3^- or SO_2[1, 34].

3.3.3 Ppy Composites and Electrical Response to CH_4 and SO_2: Effect of 13X Content

Figure 3 shows the electrical conductivity values of Ppy_ud/13X and Ppy_1:6/13X in air vs. molecular sieve 13x content. The electrical conductivity decreases with increasing 13X content as more of the insulating material is added to the composite. The electrical conductivity values of Ppy_ud/13X and Ppy_1:6/13X in N_2 also decrease with increasing 13X content, as can be seen in Table1.

Figure 4 shows the electrical sensitivity values of Ppy_ud/13X and Ppy_1:6/13X in CH_4 vs. molecular sieve 13X content. The sensitivity values of these composites to CH_4 only vary between –0.05 to 0.05. Therefore, we conclude that molecular sieve 13X does not interact with CH_4 nor improve the sensitivity of Ppy to CH_4.

Figure 5 shows the electrical conductivity sensitivity values of Ppy_ud/13X and Ppy_ud/13X in SO_2 vs. molecular sieve 13X content. The sensitivity values of these composites increase with molecular sieve 13X content and reaches a maximum and around 10 % v/v. Beyond this volume fraction, the sensitivity values decrease monotonically with molecular sieve 13x content. Sensitivity data are tabulated in Table 2.

The possible interaction between SO_2 and 13X may be identified as the electrostatic force between SO_2 and the molecular sieve 13X flamework and the electrostatic force between SO_2 and Na^+, similar to the well established interaction between CO and zeolite[24]. This interaction induces a larger quantity of SO_2 to contact the surface of Ppy, resulting in a larger number of charge carriers produced and hence a higher sensitivity. However, more 13X content is added, its presence may reduce the available contact area between SO_2 and Ppy, and hence a lower sensitivity. FTIR spectra of molecular sieve 13X were taken, as shown in Figure 2(b), before molecular sieve 13X was exposed to SO_2, and after molecular sieve 13x was exposed to SO_2 for a duration of 3 hours. The characteristic peak of the S=O asymmetric stretching at 1395 cm^{-1} does not appear in both spectra. This suggests that the interaction between SO_2 and 13X is not permanent. However after SO_2 is removed and replaced by N_2, $\Delta\sigma$'s of all composites studied do not return completely

to zero. For example, the percentages of permanent electrical conductivity change of Ppy_ud in N_2 after SO_2 removal relative to the initial electrical conductivity values in N_2 are18.2, 25.9 and 7.6% for Ppy_ud/13X-Na[100]_10, Ppy_ud/13X-Na[100]_20, and Ppy_ud/13X-Na[100]_40, respectively. Therefore, the electrical conductivity response of our composites to SO_2 is not completely reversible.

3.3.4 Ppy Composites Electrical Response to SO_2: Effect of Cation Type

The effect of cation type in 13X on electrical sensitivity of Ppy_ud/13X and Ppy_1:6/13X composites is investigated next. Molecular sieve 13X initially contained 100 % mole Na^+. After successive ion-exchanged processes, Na^+ is replaced with either Li^+, K^+, and Cs^+. Here, we shall report the results of the undoped PPy composites with 100 mole % Na^+, 50 mole % Li, 50 mole % K^+, and 50 mole % Cs^+, all having the molecular sieve 13x content of 10 % v/v. Figure 6 shows the electrical sensitivity values of the composites Ppy_ud/13X-Na[100]_10, Ppy_ud/13X-Li[50]_10, Ppy_ud/13X-K[50]_10, and Ppy_ud/13X-Cs[50]_10. The electrical sensitivity values are 0.40 ± 0.12, 0.17 ± 0.08, 0.21 ± 0.03, and 0.22 ± 0.08, respectively. Similar results are obtained for the doped Ppy_1:6 composites whose sensitivity values are tabulated in Table 2. Therefore, it appears that the composites of the Ppy_ud and Ppy_1:6 with unmodified 13X, having only Na^+, give the highest electrical conductivity sensitivity to SO_2. As the cation-exchanged molecular sieve 13x's are used to replace the unmodified 13X, the sensitivity to SO_2 is reduced in this decreasing order: Ppy_ud/ 13X-Cs[50]_10, Ppy_ud/13X-K[50]_10, and Ppy_ud/13X-[50]_10. We may note that from the expected binding energies between the cations and the CO molecule, calculated by the standard cluster model in which $AlH(OH_3)^-$, CO and alkali cations are present, the decreasing order of the binding energy is Li^+, Na^+, K^+, and Cs^+[24].

3.3.5 Ppy Composites Electrical Response to SO_2: Effect of Cation Concentration

Next, we study the effect of cation concentration in molecular sieve 13X on the electrical sensitivity of undoped PPy composites to SO_2. Ppy_ud powder was

mixed with molecular sieve13X having Li^+ contents of 30, 50, 70 and 80 mole % to form Ppy_ud/13X-Li[0]_10, Ppy_ud/13X-Li[30]_10. Ppy_ud/13X-Li[50]_10, Ppy_ud/13X-Li[70]_10, and Ppy_ud/13X-Li[80]_10. Figure 7 shows the sensitivity value of the composites as a function of Li^+ content. The electrical conductivity sensitivity is reduced as Li^+ concentration in molecular sieve13X increases. The unmodified 13X composite, containing only Na^+, has the highest sensitivity. When Na^+ is replaced by the other alkali cations, the sensitivity of the composites decreases, regardless of the alkali cation type.

3.3.6 The Temporal Response Times

The induction time is defined as the time required for the electrical conductivity to reach its equilibrium value when exposed to SO_2. The induction time of most Ppy-ud composites are longer than those of ppy_1:6 samples. For example the induction times of Ppy_ud, Ppy_ud/13X-Na[100]_10, Ppy_1:6, and Ppy_1:6/13X-Na[100]_10 are 44, 95, 24 and 68 minutes, respectively. The induction time is directly related to the accessibility and the number of available attack sites for SO_2. For Ppy_1:6 composites, the induction time decreases with increasing 13X content; it decreases 68, 60 to 34 minutes as molecular sieve13X increases from 10,20, to 40 %v/v, respectively. Table 2 lists other SO_2 induction times found. We find that there is no correlation between the induction time and the cation type or the cation concentration.

The recovery time is defined as the time required for the electrical conductivity to reach its equilibrium value when SO_2 is removed during the evacuation. It varies between 5 to 12 minutes amongst Ppy composites studied.

4. Conclusion

Undoped polypyrrole and polypyrole doped with β naphthalene sulfonic acid show no response to 10 % CH_4 , 10 % CO_2 and 1000 ppm CO. However, they respond positively to 1000 ppm SO_2 due to the electrophilic gas interaction. As the polymers are mixed with the molecular sieve 13X and exposed to 10% CH_4,

Ppy_ud/13X and Ppy_1:6/13X composites do not respond at all to CH_4. As 13X content increases, the electrical conductivity values in air and N_2 of the composites decrease. Ppy_ud/13X and Ppy_1:6/13X composites at 10% v/v of 13X content have the highest sensitivity to SO_2; the sensitivity is reduced as 13X content increases. The effect of cation type, by changing from Na^+ to Li^+, K^+, and Cs^+, and the effect of cation concentration in zeolite 13X are also studied. The composites of unmodified 13X in which Na^+ is fully present give the greatest sensitivity to SO_2. The sensitivity of Ppy/13X composite to SO_2 is reduced by exchanging cation in 13X from Na^+ to other alkali cations in this decreasing order: Cs^+, K^+, and Li^+.

5. Acknowledgements

References

(1) Prissnaroon, W.; Ruangchuay, L.; Sirivat, A.; J. Schwank, J. *Synth. Metals.* **2000**, 114, 65-72.

(2) Kohlman, R.S.; Joo, J.; Epstein, A.J. *Physical Properties of Polymer Handbook*; Woodbury: The United State of America, 1996; Chapter 34.

(3) Ruangchuay, R.; Sirivat A.; Schwank, J. *Synth. Metals.* **2003**, 117, 1-7.

(4) Nechtschein, M.; Devreux, F.; Genoud, F. *Synth. Metals.* **1986**,15, 59-78.

(5) Fink, J.; Scheerer, B.; Wernet, W.; Monkenbusch, M.; Wegner, G.; Freund, H-J.; Gonska, H. *Physical Review B.* **1986**, 34, 1101-1115.

(6) Bätz, P.; Schmeisser, D.; Göpel, W. *Phys. Rev. B.* 1991,43, 9178-9189.

(7) Thiéblemont, J.C.; Brun, A.; Marty, J.; Planche, M.F.; Calo, P. *Polymer*, **1995**,36,1605-1610.

(8) Appel, G.; Yfantis, A.; Göpel, W.; Schmeißer, D. *Synth. Metals.* **1996**, 83, 197-200.

(9) Shen, Y.; Wan, M. *J. Pol. Sci. A: Polymer Chemistry.* **1997**, 35, 3689-3695.

(10) Cassignol, C.; Oliver, P.; Richard, A. *J. Appl. Pol. Sci.* **1991**, 70,1567-1577.

(11) Benseddik, E.; Makhlouki, M.; Bernede, J.C.; Lefrant, S.; Proń, A. *Synth. Metals,* **1995**, 72, 237-242.

(12) Heurberger, H.; Tresch, S.; Dietler, G. *Thin Solid Films.* **1995**, 271, 144-146.

(13) Cheah, K.; Forsyth, M.; Truong, V-T; Olsson-Jacques, C. *Synth. Metals.* **1997**, 84, 829-830.

(14) Brie, M.; Turcu, R.; Neamtu, C.; Pruneanu, S. (1996). *Sensors and Actuators B.* **1996**, 37,119-122.

(15) Child, A.D.; Kuhn, H.H. *Synth. Metals.* **1997**, 84, 141-142.

(16) Gilani, T.H.; Ishiguro, T. *Synth. Metals.* **1997**, 84, 845-846.

(17) Fedorko, P.; Skákalová, V. *Synth Metals.* **1998**, 94, 279-283.

(18) Cheah, K.; Forsyth, M.; Truong, V-T. *Synth. Metals.* **1999**, 101, 19.

(19) Ando, E.; Onodera, S.; Iino, M.; Ito, O. *Carbon.* **2001**, 39, 101-108.

(20) Hay, N.E. *Natural Gas Aplications for Air Pollution Control*, The Fairmont Press, Inc.: The United State of America, 1987; Chapter 3.

(21) Chang, R. *Chemistry*, McGraw-Hill :The United State of America, 1994.

(22) O'Neill, P. *Environmental Chemistry*, 2 nd ed.; Chapman and Hall: The United State of America, 1993; Chapter 5-6.

(23) Chuapradit, C.; Wannatong, L.R.; Chotpattananont, D.; Sirivat, A.; Schwank, J. Submitted to *Polymer*.

(24) Ferrari, A.M.; Neyman, K.M.; Rösch, N.*J. Phys. Chem.B.* **1997**, 101, 9292-9298.

(25) Li, P.; Xiang, Y.; Grassian, V.H.; Larsen, S.C. *J. Phys. Chem.B.* **1999**, 103, 5058.

(26) Densakilprasert, N.; Wannatong, L.R.; Chotpattananont, D.; Hiamtup, P.; Sirivat A.; Schwank, J. Submitted to *Mat. Sci. and Eng.* .

(27) Bogang, T.; Zerbi, G. *Synth. Metals.* **1989**, 28, C1-C6.

(28) Khulbe, K.C.; Mann, R.S. *J. Pol. Sci.: Polymer Chemistry Edition.* **1982**, 20,1089-1095.

(29) Kang, H.C; Geckeler, K.E. *Polyme.*, **2000**, 41, 6931-6934.

(30) Shen, Y.; Wan, M. *Synth. Metals.* **1998**, 96, 127-132.

(31) Street, G.B.; Clarke, T.C.; Krounbi, M.; Kanasawa, K.; Lee, V.; Pfuger, P.; Scott, J.C.; Weiser, G. *Mol. Cryst.Liq.Cryst.* **1982**, 83, 253-264.

(32) Gassner, F.; Graf, S.; Merz, A. *Synth. Metals.* **1997**, 87, 75-79.

(33) P.W. Atkins, P.W. *Physicals Chemistry*, 5th ed.; Oxford University Press: Great Britain, 1995; Appendices.

(34) Silverstien, R.M.; Bassler, G.C.; Morrill, T.C. *Spectrometric Identification of Organic Compounds*, 5th ed.; John Wiley & Son: The United State of America, 1991, 129.

CAPTION OF TABLES

Table1 The Ppy/zeolite13X samples and their % apparent doping levels (DL), % degrees of crystallinity (DC), the induction times (t_i), the recovery time (t_{re}), electrical conductivity values in air, N_2, 10%methane, 10%CO_2, and1000 ppm CO and the electrical response ($\Delta\sigma/\sigma_{N2}$) upon exposed to 10 %methane, 10% CO_2 and 1000 ppm CO at 28 °C, at atmospheric pressure

Table 2 The Ppy/zeolite13X samples and their % apparent doping levels (DL), % degrees of crystallinity (DC), the induction times (t_i), the recovery time (t_{re}), electrical conductivity values in air, electrical conductivity values in N_2, electrical conductivity values in SO_2 and the electrical response ($\Delta\sigma/\sigma_{N2}$) upon exposed to 1000 ppm SO_2 /NO_2 mixture at 28 °C, at atmospheric pressure

CAPTION OF FIGURES

Figure 1 The electrical conductivity of polypyrrole at various N_d/N_m.

Figure 2 The FTIR spectra of ;a) Ppy_ud, b) molecular sieve13X: before the SO_2 exposure (solid line) and after the SO_2 exposure (broken line).

Figure 3 The electrical conductivity of Ppy_ud and Ppy_1/6 at various 13X content.

Figure 4 The electrical response of Ppy_ud and Ppy_1/6 to methane at various 13X content.

Figure 5 The electrical sensitivity of Ppy/13X composite at various 13X content.

Figure 6 The electrical sensitivity of Ppy/13X of various cation type: Na[100], Li[50], K[50], and Cs[50] to 1000 ppm SO_2.

Figure 7 The electrical sensitivity of Ppy13X composites of various Li^+ concentrations to 1000 ppm SO_2.

Table 1 The Ppy/zeolite13X samples and their % apparent doping levels (DL), % degrees of crystallinity (DC), the induction times (t_i), the recovery time (t_{re}), electrical conductivity values in air, N_2, 10%methane, 10%CO_2, and1000 ppm CO and the electrical response ($\Delta\sigma/\sigma_{N2}$) upon exposed to 10 %methane, 10% CO_2 and 1000 ppm CO at 28 $^{\circ}$C, at atmospheric pressure

sample	DL	DC	t_i	t_{re}	σ (S/cm)			$\Delta\sigma$	$\Delta\sigma/\Delta\sigma_{N2}$
			(min)	(min)	air	N_2	Methane	(S/cm)	
Ppy_ud	0.26	54.3	80	5	$(4.68\pm2.48) \times 10^{-1}$	$(3.96\pm3.36) \times 10^{-1}$	$(3.97\pm3.44) \times 10^{-1}$	$(6.00\pm4.78) \times10^{-3}$	$(1.57\pm0.11) \times 10^{-2}$
Ppy_ud/13X_5	0.26	54.3	26	17	$(1.12\pm0.49) \times 10^{-1}$	$(1.07\pm 0.52) \times 10^{-1}$	$(1.09\pm0.47) \times 10^{-1}$	$(2.06\pm4.49) \times 10^{-3}$	$(3.32\pm5.80) \times 10^{-2}$
Ppy_ud/13X_20	0.26	54.3	46 ± 26	10	$(8.62\pm.01) \times 10^{-2}$	$(6.19\pm3.02) \times 10^{-2}$	$(6.17\pm3.00) \times 10^{-2}$	$(-2.05\pm2.70) \times 10^{-4}$	$(-2.56\pm3.11) \times 10^{-3}$
Ppy_ud/13X_40	0.26	54.3	42	13	$(1.09\pm0.34) \times 10^{-2}$	$(2.82\pm1.37) \times 10^{-3}$	$(2.78\pm1.35) \times 10^{-3}$	$(-4.62\pm1.56) \times 10^{-5}$	$(-1.71\pm0.29) \times 10^{-2}$
Ppy_1:6	0.51	80.4	23 ± 3	5	3.01 ± 2.08	3.17 ± 2.31	3.17 ± 2.30	$(3.31\pm2.22) \times 10^{-3}$	$(1.06\pm0.01) \times 10^{-3}$
Ppy_1:6/13X_10	0.51	80.4	15	-	1.40 ± 0.23	1.41 ± 0.24	1.40 ± 0.22	$(-1.58\pm1.44) \times 10^{-2}$	$(-1.05\pm0.84) \times10^{-2}$
Ppy_1:6/13X_20	0.51	80.4	28	12	1.00 ± 0.13	$(9.72\pm1.59) \times 10^{-1}$	$(9.80\pm1.50) \times 10^{-1}$	$(-2.05\pm2.70) \times 10^{-4}$	$(1.26\pm1.20) \times 10^{-2}$
Ppy_1:6/13X_40	0.51	80.4	29 ± 1	17 ± 3	$(4.79\pm0.20) \times 10^{-1}$	$(2.58\pm0.20) \times 10^{-1}$	$(2.54\pm0.20) \times 10^{-1}$	$(-3.60\pm0.06) \times 10^{-3}$	$(-2.56\pm3.11) \times 10^{-3}$
					air	N_2	CO_2		
Ppy_ud	0.26	54.3	25	10	$(4.01\pm1.87) \times 10^{-2}$	$(1.98\pm0.68) \times 10^{-2}$	$(1.95\pm0.69) \times 10^{-2}$	$(-3.44\pm0.84) \times 10^{-4}$	$(-1.93\pm1.08) \times 10^{-2}$
Ppy_1:6	0.51	80.4	14	6	$(8.27\pm1.17) \times 10^{-1}$	$(5.88\pm3.49) \times 10^{-1}$	$(5.86\pm3.51) \times 10^{-1}$	$(-2.36\pm2.20) \times 10^{-3}$	$(-6.23\pm7.45) \times 10^{-3}$
					air	N_2	CO		
Ppy_ud	0.26	54.3	30	7	$(2.31\pm0.50) \times 10^{-1}$	$(1.75\pm0.11) \times 10^{-1}$	$(1.71\pm0.15) \times 10^{-1}$	$(-3.89\pm4.33) \times 10^{-3}$	$(-2.30\pm2.61) \times 10^{-2}$
Ppy_1:6	0.51	80.4	22	5	1.62 ± 0.77	1.27 ± 0.50	1.20 ± 0.49	$(-6.64\pm1.21) \times 10^{-2}$	$(-5.48\pm1.22) \times 10^{-2}$

Table 2 The Ppy/zeolite13X samples and their % apparent doping levels (DL), % degrees of crystallinity (DC), the induction times (t_i), the recovery time (t_{re}), electrical conductivity values in air, electrical conductivity values in N_2, electrical conductivity values in SO_2 and the electrical response ($\Delta\sigma/\sigma_{N2}$) upon exposed to 1000 ppm SO_2 /NO_2 mixture at 28 ^{o}C, at atmospheric pressure

| Sample	DL	DC	t_i (min)	t_{re} (min)	σ (S/cm) air	σ (S/cm) N_2	σ (S/cm) SO_2	$\Delta\sigma$ (S/cm)	$\Delta\sigma/\sigma_{N2}$
Ppy_ud	0.26	54.3	44±6	8±2	$(4.74\pm3.00) \times 10^{-1}$	$(2.71\pm0.13) \times 10^{-1}$	$(3.38\pm0.44) \times 10^{-1}$	$(6.71\pm3.10) \times 10^{-2}$	$(2.46\pm1.02) \times 10^{-1}$
Ppy_ud/13X-Na[100]_10	0.26	54.3	95±7	11±1	$(5.21\pm0.09) \times 10^{-2}$	$(2.78\pm0.80) \times 10^{-2}$	$(3.86\pm0.80) \times 10^{-2}$	$(1.09\pm0.01) \times 10^{-2}$	$(4.00\pm1.16) \times 10^{-1}$
Ppy_ud/13X-Na[100]_20	0.26	54.3	52±1	5	$(3.11\pm0.52) \times 10^{-2}$	$(2.97\pm1.53) \times 10^{-2}$	$(3.55\pm1.67) \times 10^{-2}$	$(5.88\pm1.33) \times 10^{-3}$	$(2.15\pm0.66) \times 10^{-1}$
Ppy_ud/13X-Na[100]_40	0.26	54.3	64±8	6±1	$(1.37\pm0.03) \times 10^{-2}$	$(1.18\pm0.23) \times 10^{-2}$	$(1.31\pm0.21) \times 10^{-2}$	$(1.23\pm0.18) \times 10^{-3}$	$(1.07\pm0.35) \times 10^{-1}$
Ppy_ud/13X-Li[30]_10	0.26	54.3	44±7	-	$(1.00\pm0.002) \times 10^{-1}$	$(8.37\pm2.69) \times 10^{-2}$	$(1.03\pm0.25) \times 10^{-2}$	$(1.92\pm0.16) \times 10^{-2}$	$(2.44\pm0.98) \times 10^{-1}$
Ppy_ud/13X-Li[50]_10	0.26	54.3	67±13	10	$(7.33\pm0.74) \times 10^{-2}$	$(4.80\pm2.51) \times 10^{-2}$	$(5.54\pm3.50) \times 10^{-2}$	$(8.90\pm7.79) \times 10^{-3}$	$(1.72\pm0.67) \times 10^{-1}$
Ppy_ud/13X-Li[70]_10	0.26	54.3	60±2	6±2	$(5.65\pm1.85) \times 10^{-2}$	$(4.21\pm3.54) \times 10^{-2}$	$(5.28\pm4.86) \times 10^{-2}$	$(1.07\pm1.32) \times 10^{-2}$	$(1.91\pm1.52) \times 10^{-1}$
Ppy_ud/13X-Li[80]_10	0.26	54.3	50±14	6	$(5.06\pm2.45) \times 10^{-2}$	$(2.00\pm1.37) \times 10^{-2}$	$(2.16\pm1.53) \times 10^{-2}$	$(1.60\pm1.55) \times10^{-3}$	$(6.96\pm2.95) \times10^{-2}$
Ppy_ud/13X-K[50]_10	0.26	54.3	102±17	12±4	$(5.06\pm2.56) \times 10^{-2}$	$(4.03\pm3.88) \times 10^{-2}$	$(4.93\pm4.82) \times 10^{-2}$	$(8.99\pm9.35) \times 10^{-3}$	$(2.07\pm0.32) \times 10^{-1}$
Ppy_ud/13X-Cs[50]_10	0.26	54.3	94±48	12±1	$(5.78\pm0.25) \times 10^{-2}$	$(1.19\pm1.03) \times 10^{-2}$	$(1.50\pm1.36) \times 10^{-2}$	$(3.05\pm3.21) \times 10^{-3}$	$(2.22\pm0.77) \times 10^{-1}$
Ppy_1:6	0.51	80.4	24±2	10	4.56±2.97	2.80±0.53	3.12±0.52	$(3.17\pm0.09) \times 10^{-1}$	$(1.15\pm0.25) \times 10^{-1}$
Ppy_1:6/13X-Na[100]_10	0.51	80.4	68±32	10	1.03±0.46	1.08±1.08	1.41±1.38	$(3.27\pm2.91) \times 10^{-1}$	$(3.38\pm0.70) \times 10^{-1}$
Ppy_1:6/13X-Na[100]_20	0.51	80.4	60±1	10±1	1.23±0.15	1.06±0.09	1.25±0.07	$(1.89\pm0.18) \times 10^{-1}$	$(1.79\pm0.33) \times 10^{-1}$
Ppy_1:6/13X-Na[100]_40	0.51	80.4	34±12	10±2	$(3.63\pm2.17) \times 10^{-1}$	$(1.33\pm0.88) \times 10^{-1}$	$(1.44\pm0.98) \times 10^{-1}$	$(1.10\pm0.94) \times 10^{-2}$	$(7.61\pm2.1) \times 10^{-2}$
Ppy_1:6/13X-Li[50]_10	0.51	80.4	33±4	-	1.49±1.26	1.51±1.30	1.67±1.45	$(1.64\pm1.52) \times 10^{-1}$	$(1.04\pm0.11) \times 10^{-1}$
Ppy_1:6/13X-K[50]_10	0.51	80.4	40±7	6	$(5.10\pm5.18) \times 10^{-1}$	$(3.83\pm3.34) \times 10^{-1}$	$(4.34\pm4.71) \times 10^{-1}$	$(5.11\pm3.70) \times 10^{-2}$	$(1.47\pm0.32) \times 10^{-1}$
Ppy_1:6/13X-Cs[50]_10	0.51	80.4	50	6±1	2.19±1.08	1.24±0.05	1.49±0.005	$(2.48\pm0.41) \times 10^{-1}$	$(2.00\pm0.40) \times 10^{-1}$

Figure 1

Figure 2   a)

wave number (cm^{-1})

Figure 2   b)

wave number (cm⁻¹)
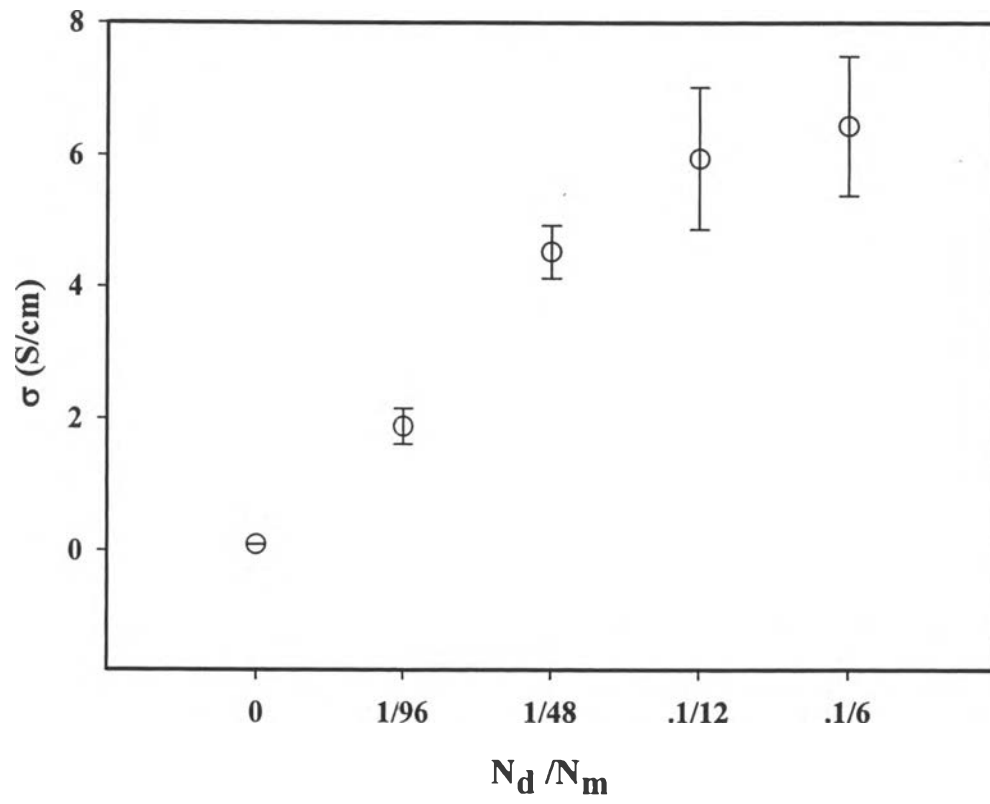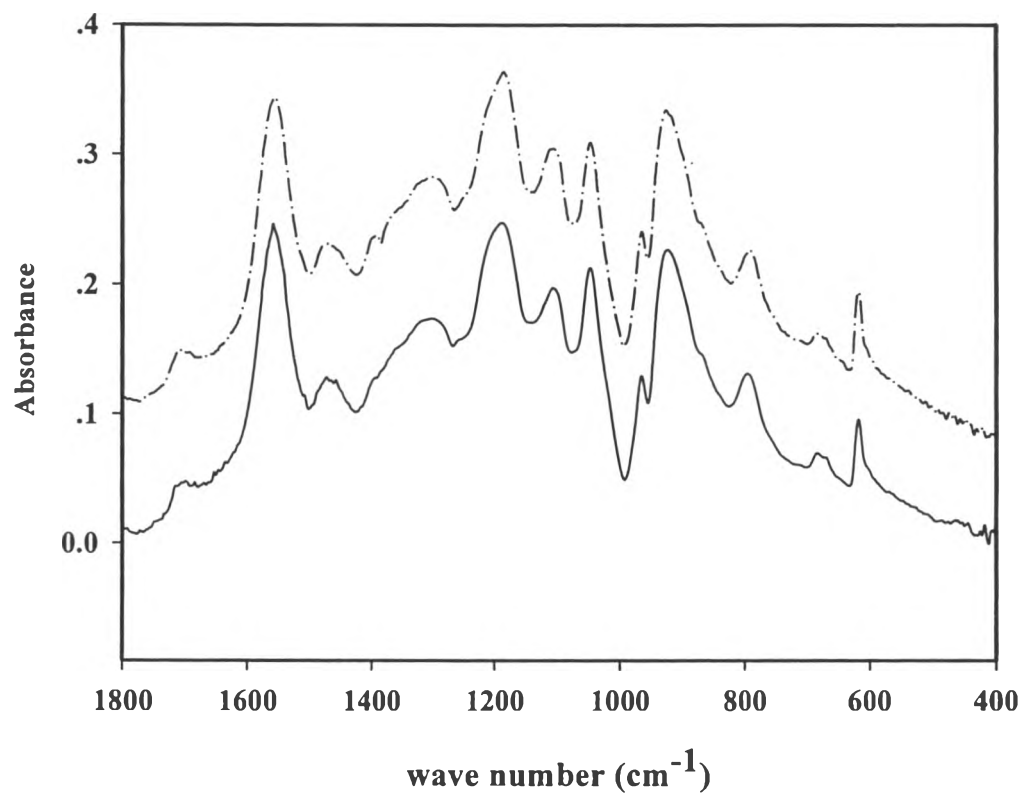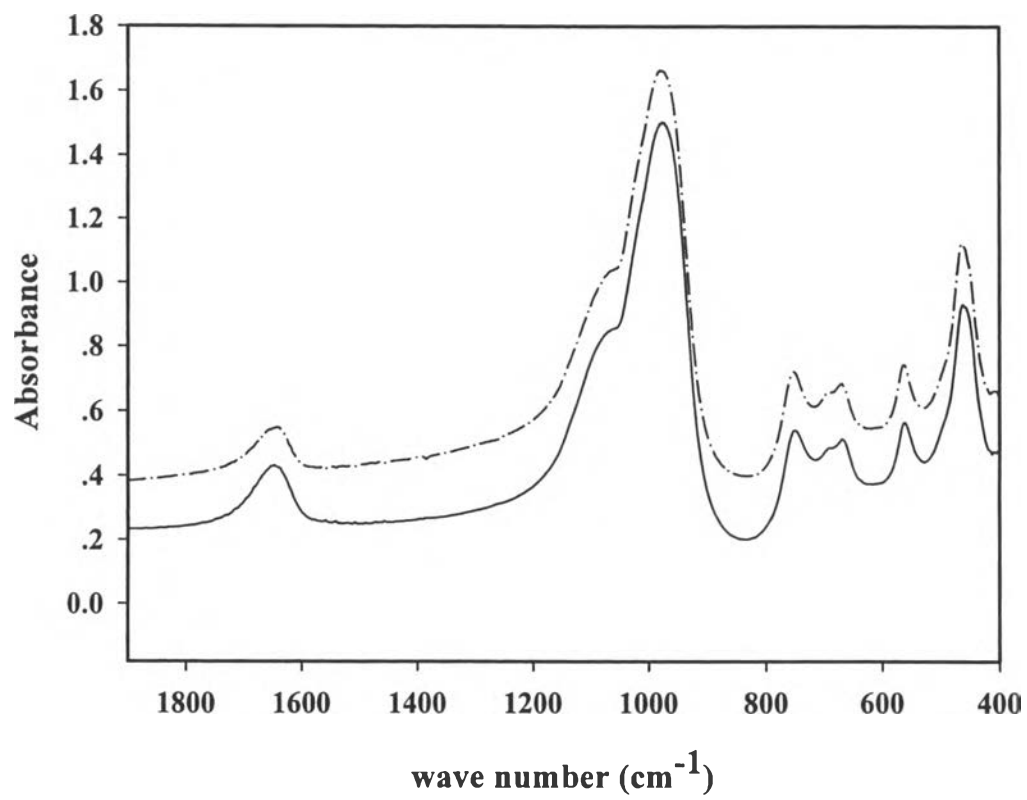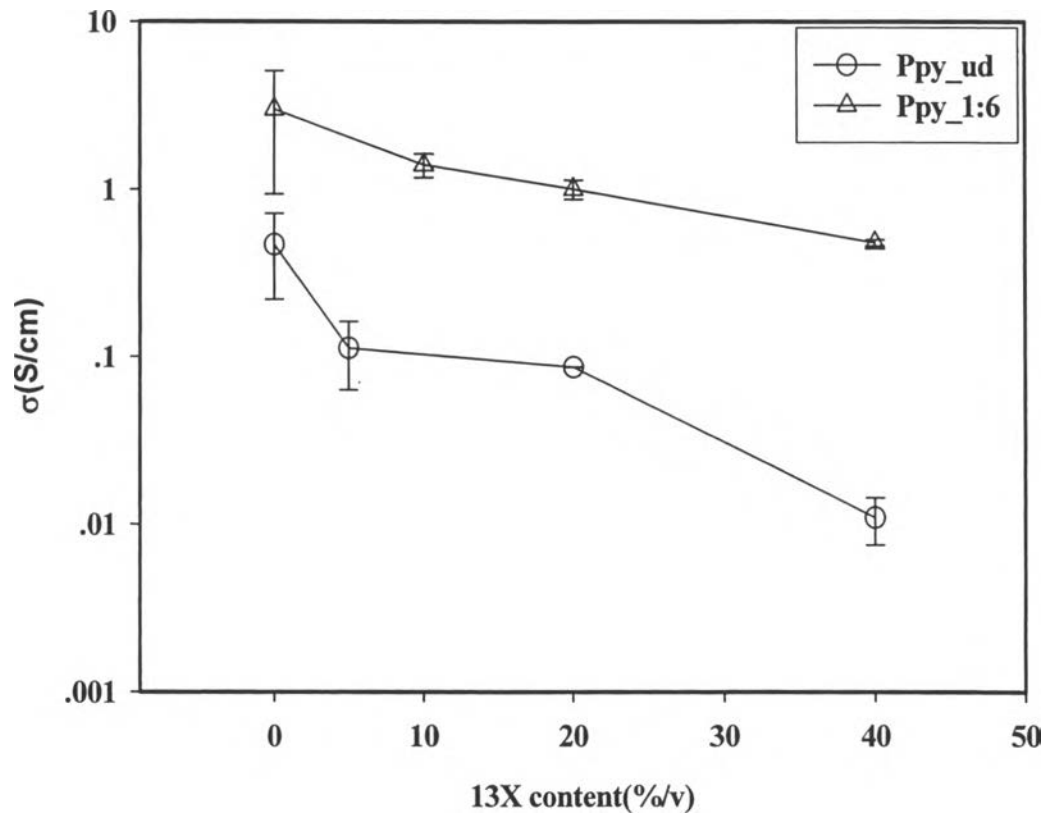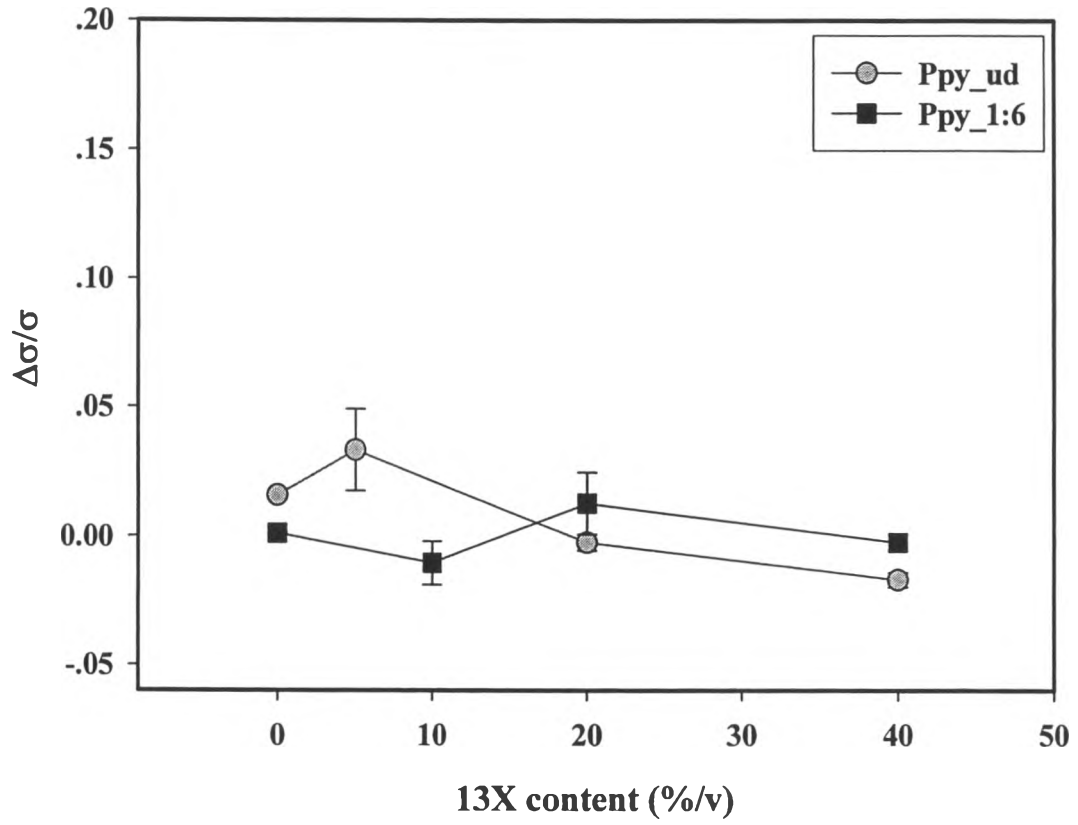
Figure 3

Figure 4

Figure 5

Figure 6

Figure 7